DYNAMIC LATERAL EARTH PRESSURES ON UNDERGROUND STRUCTURES: PREDICTING STRESSES DUE TO IMPACT LOADINGS

Presented to the Following Faculty from The University of

Texas at San Antonio Civil Engineering Department:

Dr. Alberto Arroyo

Dr. Jose Weissman

Dr. Chia S. Shih

Dr. Asadul Chowdhury

In Coordination with Dr. Sam Helwany, Assistant Professor at the University of Wisconsin at Milwaukee Civil Engineering Department

By:

Major Curt A. Van De Walle, USAF

REPORT DOCUMENTATION PAGE	Form Approved OMB No. 0704-0188

1. AGENCY USE ONLY *(Leave blank)*	2. REPORT DATE 8.Nov.99	3. REPORT TYPE AND DATES COVERED MAJOR REPORT

4. TITLE AND SUBTITLE
DYNAMIC LATERAL EARTH PRESSURES ON UNDERGROUND
STRUCTURES: PREDICTING STRESSES DUE TO IMPACT LOADINGS

5. FUNDING NUMBERS

6. AUTHOR(S)
CAPT VAN DEWALLE CURT A

7. PERFORMING ORGANIZATION NAME(S) AND ADDRESS(ES)
UNIVERSITY OF TEXAS SAN ANTONIO

8. PERFORMING ORGANIZATION REPORT NUMBER

9. SPONSORING/MONITORING AGENCY NAME(S) AND ADDRESS(ES)
THE DEPARTMENT OF THE AIR FORCE
AFIT/CIA, BLDG 125
2950 P STREET
WPAFB OH 45433

10. SPONSORING/MONITORING AGENCY REPORT NUMBER
FY99-432

11. SUPPLEMENTARY NOTES

12a. DISTRIBUTION AVAILABILITY STATEMENT
Unlimited distribution
In Accordance With AFI 35-205/AFIT Sup 1

12b. DISTRIBUTION CODE

13. ABSTRACT *(Maximum 200 words)*

14. SUBJECT TERMS

15. NUMBER OF PAGES

16. PRICE CODE

17. SECURITY CLASSIFICATION OF REPORT	18. SECURITY CLASSIFICATION OF THIS PAGE	19. SECURITY CLASSIFICATION OF ABSTRACT	20. LIMITATION OF ABSTRACT

TABLE OF CONTENTS

TABLE OF FIGURES

INDEX OF TABLES

ABSTRACT

The underground detonation of an explosive device produces shock waves such as Primary waves (P-waves) and Secondary (or Shear) waves (S-waves). These waves cause buildup of pressures within a soil medium. These pressures have the capability of rendering destructive forces on underground structures, and consequently represent life-threatening danger. Understanding these forces can aid in the design of underground structures to withstand such pressures, or alternatively, to design munitions which will render the maximum destructive power on underground structures when dropped at a predefined depth and distance from the structure. A conceptual representation of dynamic lateral earth pressures generated from an earth-penetrating munition is shown in Figure 1.
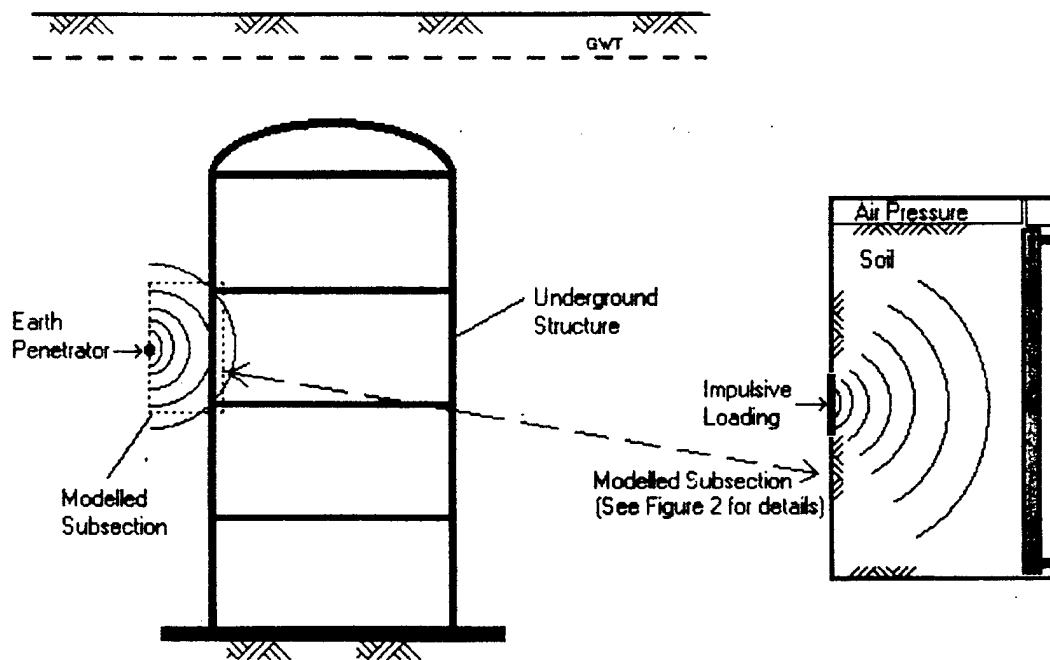
Figure 1 - *Conceptual Representation of Underground Dynamic Lateral Forces*

Many tests have analyzed the effects of an impulse loading on a soil sample.   The

present paper analyzes one such test conducted at the University of Texas at San Antonio

(UTSA) in August 1998 under the supervision of Dr. Sam Helwany, and comments on

the ability to predict free field stresses within a soil sample given the loading, loading

duration, and distance from the loading within the soil sample. In order to do this, it is

also necessary to discuss the small deflection theory of bending of plates with regards to

the targeted wall within the soil sample.

INTRODUCTION

The objective of this special project is to analyze the ability to predict the stresses and

strains generated on an underground structure at a given distance from a known impact

loading, similar to that which might be generated by a bomb blast. This project is part of

Phase I of a larger study funded by the United States Air Force (USAF) entitled

"Dynamic Lateral Earth Pressure on Underground Structures."   This study was initiated

by Dr. Sam Helwany, formerly of the UTSA Engineering Division and presently at the

University of Wisconsin at Milwaukee; Dr. Ronald Bagley of the UTSA Engineering

Division; and Dr. Asadul Chowdhury, Southwest Research Institute and adjunct faculty

with the UTSA Division of Engineering.

This special project also utilized research conducted by Dr. Hung-Liang (Roger) Chen et.

al. at the University of West Virginia regarding "Dynamic Responses of Shallow-Buried

Flexible Plates Subjected to Impact Loading" published in The Journal of Structural

Engineering, January 1996. Dr. Chen's research analyzed a modified version of

Boussinesq's Equation (1883) developed to predict the free field stresses in a soil mass

generated by an impact loading. These predictions, together with predictions developed

from a decoupled Single Degree of Freedom (SDOF) model, were compared with results measured in laboratory experiments. The present paper further analyzes the ability to predict stresses by comparing measurements gained experimentally in the UTSA test to those predicted by the formula.

TEST CONDITIONS

In order to test the effect of impact loading on an underground structure, a large-scale impulse test was performed at UTSA in August 1998. The model used for this test can be found at Figure 2. The load was provided by a MTS Impulse Generator capable of applying an impulse load of 3500 pounds within 5 milliseconds at an estimated velocity of 100 inches/second. The box itself was constructed of steel. The front plate was made of 1/2 inch steel plate with an 11.5 inch diameter suspended cutout, upon which the load was applied. The target plate and top were made of 1/2 inch aluminum plate, and the sides and bottom were made of 1/8 inch steel plate. All corners of the box were reinforced with 1/2 inch steel straps. The box was rigidly connected to a strong wall. An air bladder was placed immediately above the soil sample, and a pressure of 10 psi was applied to simulate a buried depth of 13.33 feet in the same soil medium. High-density foam was then placed between the air bladder and the top of the box to act as a rigid spacer.

The target plate was heavily instrumented with accelerometers and strain gauges in addition to load cells located at each corner. Due to symmetry, only one side of the plate was instrumented. This analysis will only deal with the strain gauges located at the center of the target plate. These gauges were selected because they represent the location of maximum stress and strain.

Legend: (1) Soil   (2) Rigid Container
         (3) Target Plate   (4) Air Bag/Spacers
         (5) MTS Impulse Generator   (6) Circular Loading Plate
         (7) Load Cell
         (11) Load Cell

Not Included: (8) Accelerometer   (9) Pressure Gauge
This Test   (10) Pore Pressure Transducer
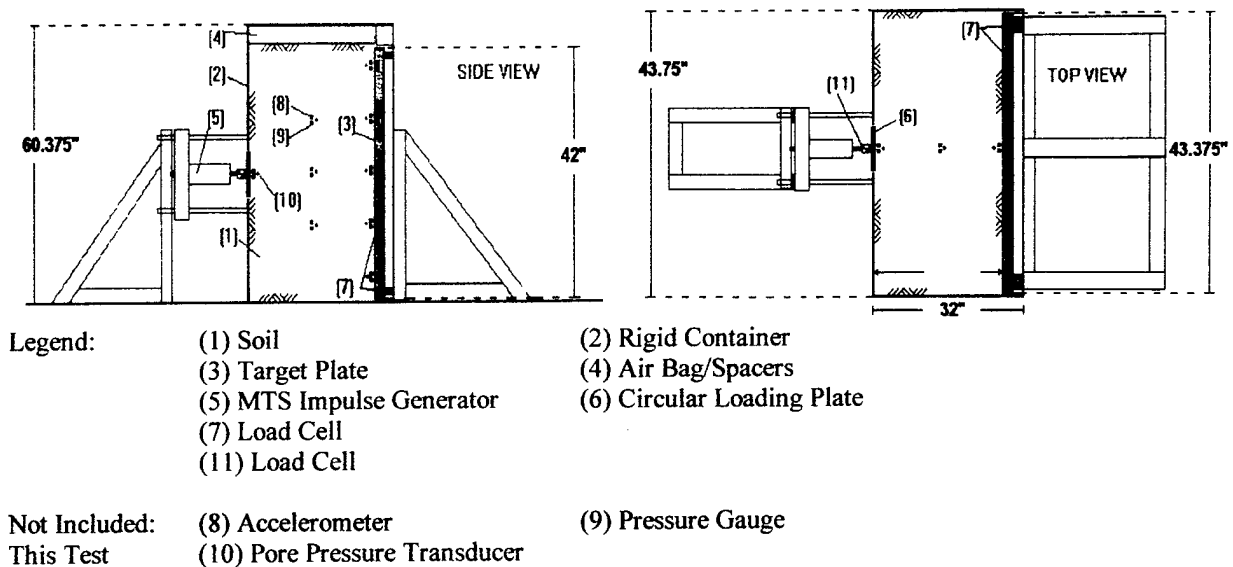
Figure 2 - *Model of Large Scale Impulse Test (Not To Scale)*

MATERIAL PROPERTIES

The soil used for this test was a Number 0 Monterrey Sand. Relative density of the sand was measured at 108 pounds per cubic foot. Two sieve analyses were performed on the sand, the results of which can be seen in Figure 3. The results of the two tests were practically identical. It can be seen that the sand is a uniformly graded medium, meaning that most of the particles are of the same size. The moisture content of the sample was negligible (e.g. - less than 2%).

Perhaps one of the most important aspects of the experiment, or at least the one which required the most attention to detail, was the alluvial deposition of the soil sample. In order to ensure a uniform sample, a device was constructed to "rain" the sand into the box. This required a uniform rate of flow deposited from a constant height. This was difficult to obtain, because the height of drop varied as the sample depth increased. In the end, a rectangular box, approximately three feet in length with a square cross-sectional ·

area was used. Each side of the cross-section was approximately one foot long. Sand was fed into the top of the box via a tube connected to a large funnel suspended over the box. As sand passed approximately two-thirds of the way through the length of the box, it passed through a grid of circular holes which spread the sand out evenly across the cross section of the box. A screen was placed at the bottom of the box to slow the fall of the sand as it left the box. The sand was rained from a constant height of four inches above the top of the soil sample. The box was moved from one end of the sample to the other and simultaneously lifted by means of a mechanical device mounted on tracks above the box. This provided a compact sample of uniform density for use in the test.
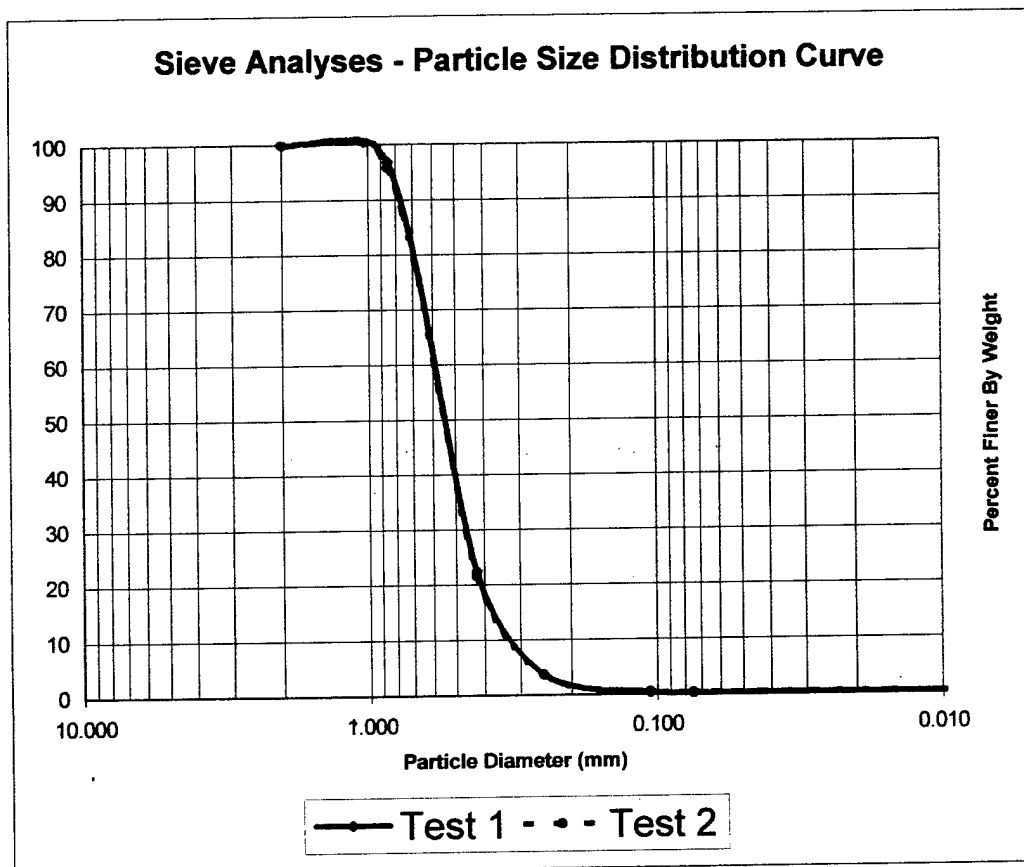
Sieve Analyses - Particle Size Distribution Curve

Figure 3 – Sieve Analyses of Soil Sample

The aluminum target plate was assumed to be isotropic and homogenous. In addition, the Young's Modulus of Elasticity, E, of the aluminum was taken as 10×10^6 psi. This is an approximate value of E for aluminum, which ranges from $9.9 - 10.3 \times 10^6$ psi. Likewise, Poisson's Ration, u, for the aluminum was taken as an average value of .332 from a range of .330-.334.

ASSUMPTIONS

Several assumptions were made for the purpose of this analysis. They are as follows:

1. Since P-waves travel faster than S-waves, the effect of S-waves can be neglected in the initial maximum strain reading. In other words, the stresses caused by waves reflecting from the boundaries do not affect the initial maximum strain reading, thereby providing a free field stress reading.

2. The side depth of the soil sample is intentionally smaller than the height and width of the sample. This reduces the effect of reflected stress waves from the boundary of the sample, more closely representing free field stress conditions.

3. The box is rigidly connected to the wall, with no lateral movement. Additionally, the rigid steel frame and the concentricity of the loading reduce the possibility of lateral movement.

4. The soil is uniformly deposited and is therefore homogenous and isotropic. This is accomplished by the use of a "raining" device previously discussed.

5. The target plate is simply supported on all edges. In actuality, the plate is pinned by the use of bolts at each of its four corners. The simply supported case, which allows for rotation but not deflection at the corners, is a close approximation to the actual conditions and represents an allowable margin of error.

6. The target plate was assumed square (42" x 42"). In actuality, the target plate was slightly rectangular (42" x 43.375").

7. Air pressure introduced into the air bag at the top of the sample represents the increased pressure on the sample with burial depth. A confining pressure of 10 psi was applied to the sample, representing a burial depth of 13.33 feet in the same sand material.

8. The friction forces between the cutout loading plate, suspended in-place by silicone sealant, are negligible when compared to the force of the impact.

LOADING AND DISPLACEMENT HISTORY

The loading and displacement history can be seen in Figure 4. The graph on the top represents the loading, while the graph at the bottom represents the displacement of the loading plate. Due to the speed of loading, a trigger mechanism had to be devised to capture the entire history. Therefore, the portion of the graph before and after the steep loading and unloading curve can be ignored, as this is due to the effect of the triggering mechanism and vibrations following impact. The actual time of loading is .021 seconds, or 21 milliseconds. The peak load over this time is 3725 pounds. The actual displacement of the loading plate, measured only during the time of loading, is .2 inches.
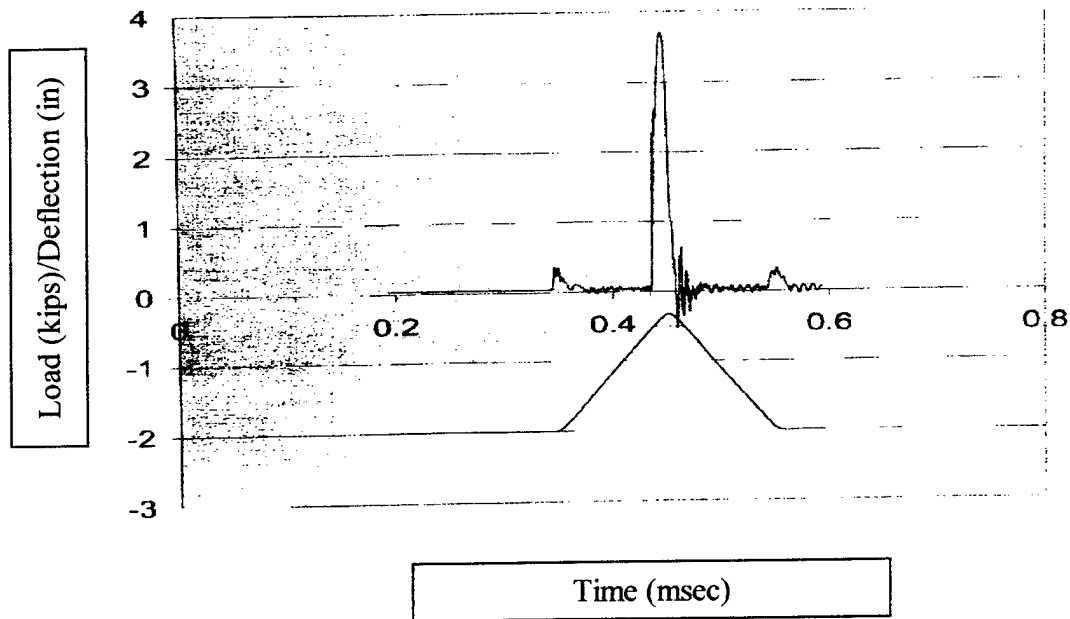
Figure 4 – *Actual Loading and Displacement History*

CALCULATION OF FREE FIELD STRESS

As mentioned above, this project utilized research conducted by Dr. Hung-Liang (Roger) Chen et. al. at the University of West Virginia in 1996. This work was published under the title "Dynamic Responses of Shallow-Buried Flexible Plates Subjected to Impact Loading" in the January 1996 edition of the Journal of Structural Engineering. Dr. Chen used the model depicted in Figure 5 in his research. A portion of this research uses an equation for predicting the free-field stresses generated by an impulse load on a soil sample by using the relationship in Equation (1).
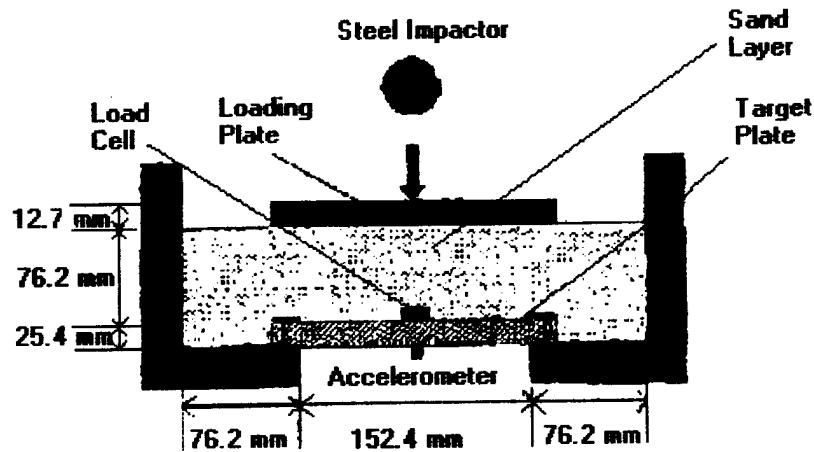
Figure 5 – *Model Used in Dr. Chen's Research*

$$\sigma_{f(t,z)} = q(t)\left[1 - \frac{z^3}{\left(a^2 + z^2\right)^{1.5}}\right] \qquad (1)$$

where: $\sigma_{f(t,z)}$ = free field stress at a distance z from the loading plate at time, t

a = radius of the loading plate

z = distance to calculated free field stress

In this case, q(t) is the approximate uniform load resulting from a point load on a rigid plate resting on an elastic half-space. It is calculated by using the equation for maximum deflection developed by previous researchers, and takes the form of Equation (2).

$$q(t) = \frac{P(t)}{4a^2} \qquad (2)$$

where: P(t) = time varying point load

- 12 -

Unlike our test, in which the impact load was measured, the impact load in Dr. Chen's study, which was applied by dropping a steel ball from a given height, was estimated. As such, the impact load was defined as a product of the loading magnitude and a time-varying function. The peak amplitude of the loading, P_o, is found by applying Equation (3) below (numbers in parentheses are those used in Dr. Chen's research). The value of P_o used in Dr. Chen's research was 1,727 lbf.

$$P_o = \frac{M_b(2gH)^{\frac{1}{2}}}{\int_0^{T_o} f(t)dt} \qquad (3)$$

where: M_b = mass of the steel ball

H = dropping height (= 24 in)

g = gravitational acceleration (= 32.2 ft/sec/sec)

$f(t)$ = time varying function (= 1.0 for $q(t)_{max}$)

T_o = total duration of impact (= .204ms)

The time varying function, $f(t)$, was approximated using a Hanning's function for a monopeak, smooth-shaped curve for a given duration in the form of:

$$f(t) = 0.5 - 0.5\cos\left(\frac{2\pi t}{T_o}\right) \qquad (4)$$

An example of this type of loading history can be seen in Figure 6. For comparison, the loading magnitude, P_o, and the duration of the impact, T_o, are assumed to be identical to those used in the UTSA experiment and the actual loading history from the UTSA test is provided for comparison.

Loading History - Assumed vs. Actual

$f(t) = 0.5 - 0.5 \cos (2\pi \, t/T_o)$

--- Actual Load ——— Assumed Load
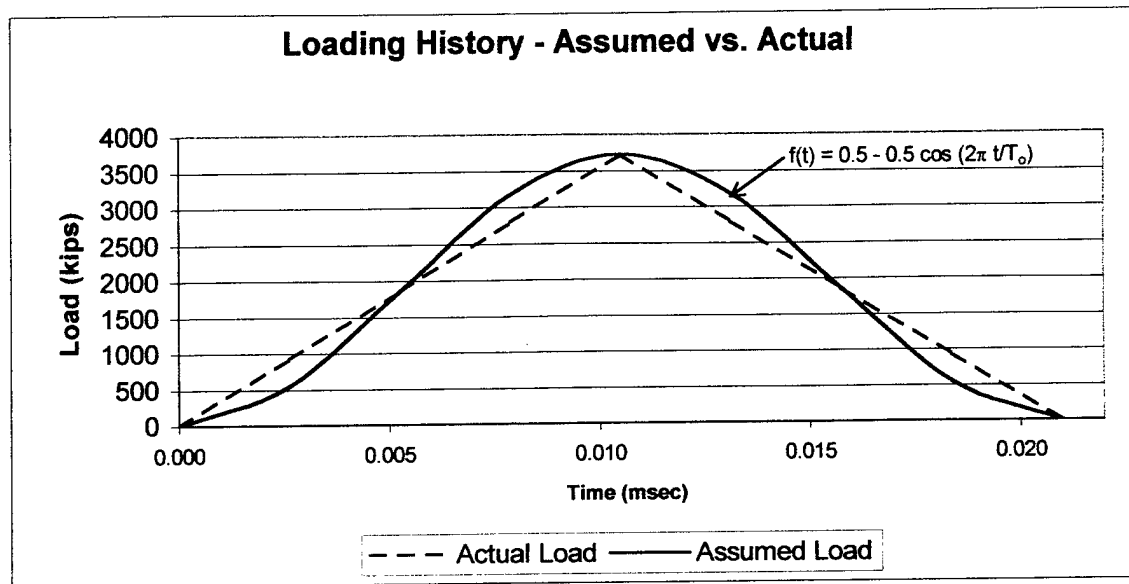
Figure 6 – *Comparison of Assumed and Actual Loading History*

MAXIMUM STRAIN ON THE TARGET PLATE

Once the free field stress was calculated, the maximum bending stress on the target plate could also be calculated. To do this requires application of the theory of bending of plates. In our case, assuming the z-direction is normal to the plate, the stress in the z-direction is assumed to be zero. Assuming the aluminum plate is isotropic and homogenous and the load is uniform in all directions, the stresses in the x- and y-directions are equal and represent the principal stresses in Mohr's circle. This example of biaxial tension is represented in Figure 7.

Figure 7 – *Mohr's Circle for Case of Biaxial Tension*

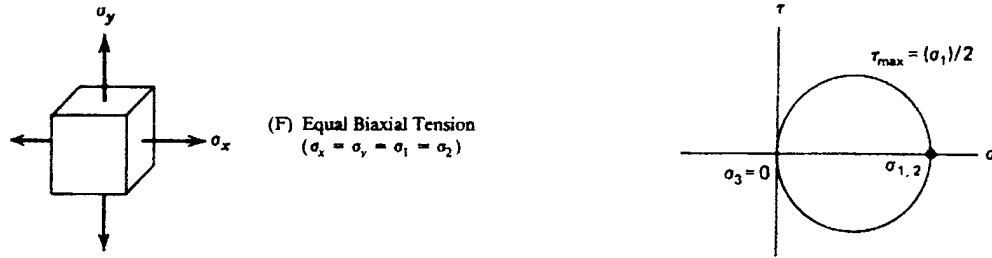The bending response of plates can be solved in a variety of ways. Analytical solutions of differential equations with given boundary conditions were the earliest solutions. Another form of solution can be obtained via numerical methods, i.e. - finite-difference and finite-element methods. In fact, Dr. Helwany will use a computer model to further analyze the stresses and strains on the target plate as a separate part of this study. For this portion of the study, however, solutions were obtained using graphical methods with constants that vary for different boundary and loading conditions. The maximum stress and maximum deflection were calculated using Equations (5) and (6), respectively.

$$\sigma_{max} = \frac{C_n pL^2}{h^2} \qquad (5)$$

$$\omega_{max} = \frac{K_n pL^4}{Eh^3} \qquad (6)$$

where: σ_{max} = maximum stress

ω_{max} = maximum deflection

p = pressure on plate

C_n = variable from Figure 8 (c)

K_n = variable from Figure 8 (d)

Other important considerations for determining the maximum stress and deflection are the actual boundary conditions and loading conditions for our test. In actuality, the target plate was suspended by bolts on each of its four corners, and was allowed to deflect freely at all other points. For analysis sake, the plate was assumed to be simply supported along all four edges, which would not allow deflection at any of the edges, but would allow rotation at all edges. This is a good approximation of actual conditions. Additionally, the loading condition on the plate was assumed to be uniform for the first analysis (Case 7 in Figure) and in the shape of a triangular prism, with the maximum load at the center for the second analysis (Case 11 in Figure). Variables for these equations were based on the dimensions of the plate, as well as the boundary and loading conditions, and were taken from the graphs shown in Figure 8.

CONVERSION OF STRESS RESULTS TO STRAIN

In order to have the results in a format that could be compared to the laboratory results, it is necessary to convert the maximum stress on the plate, which occurs at the extreme fiber at the center of the plate, to maximum strain. If all previous assumptions are correct, the stresses and strains in both the x- and y- directions are equal, and only the equation for ε_x will be given. Equation (7), based on Hooke's Law, is applied to determine the strain.

$$\varepsilon_x = \frac{\sigma_x - \upsilon\left(\sigma_y + \sigma_z\right)}{E} \qquad (7)$$
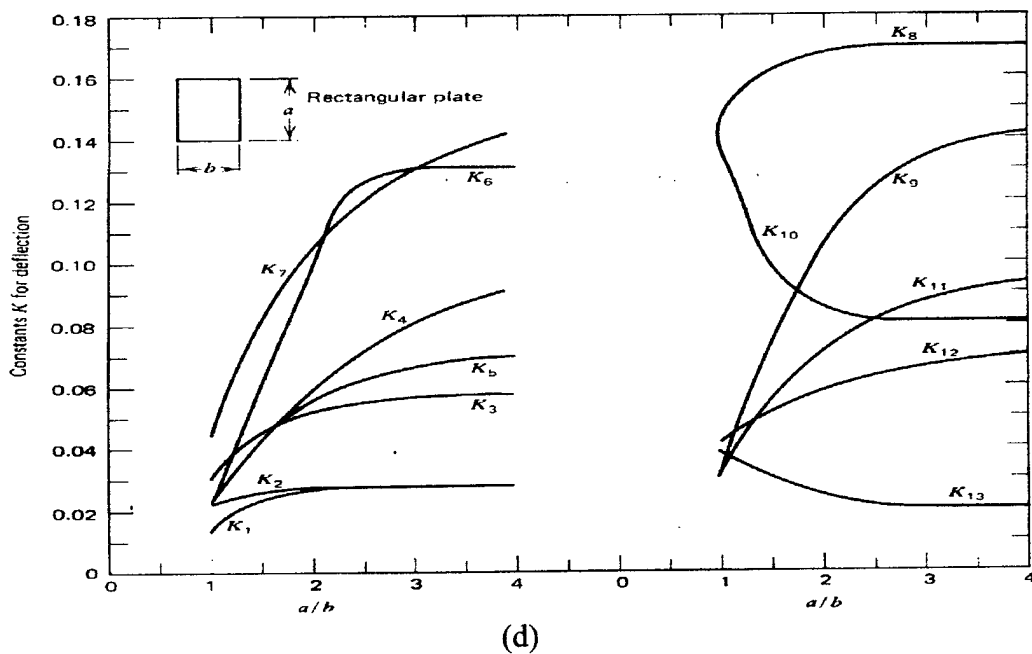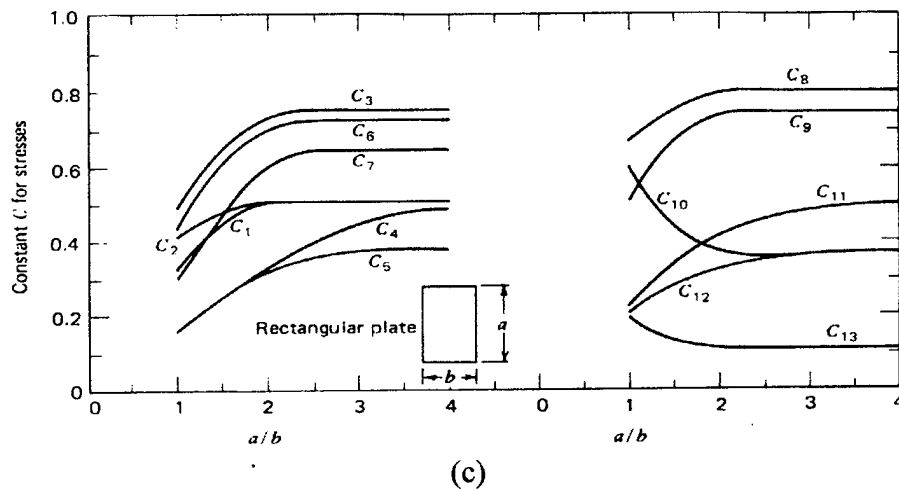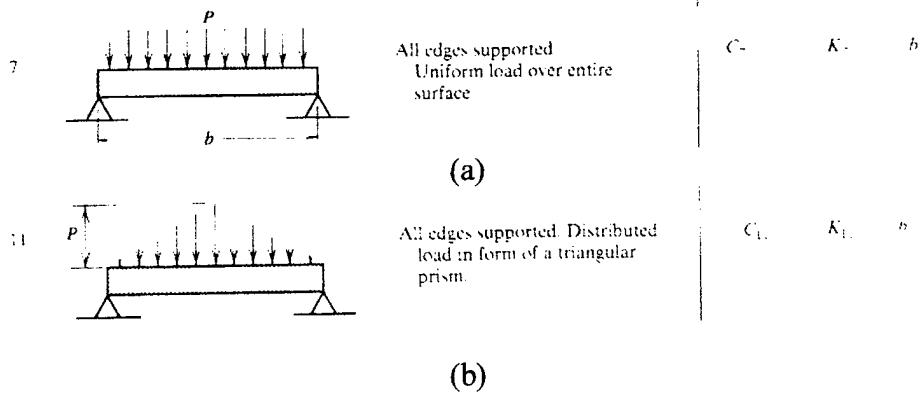
Figure 8 – Determining Maximum Stress and Deflection on a Rectangular Plate:
(a) Case of Uniform Load   (b) Case of Triangularly Distributed Load   (c&d)
Variables for Calculating the Max Stress/Deflection

In the case of equal biaxial tension, with stresses in the x- and y- directions equal and normal stresses and strains zero, Hooke's Lay reduces to Equation (8).

$$\varepsilon_x = \frac{\sigma_x(1-\upsilon)}{E} \qquad (8)$$

RESULTS

The stress, deflections and strain were calculated using the above equations for the UTSA test for each of the cases listed above and are shown in Table 1 below. From this point on, discussion will be limited to Case 2, the case of the triangular load shape, as it more closely represents the actual UTSA test conditions.

	Case 1 - Uniform Pressure	Case 2 - Non-Uniform Pressure
Max. Stress	3192 psi	2309 psi
Max. Deflection	.165 in.	.116 in.
Max. Strain (%)	.02132	.01542

Table 1 – *Calculated Stress, Deflection and Strain for the UTSA Test*

One interesting point to note is that the maximum deflection for the target plate is on the right order of magnitude for each case. The measured deflection of the loading plate was .2 inches. This implies that some of the loading was absorbed by the damping characteristic of the sand, which is reflected in smaller deflections of the target plate.

COMPARISON OF RESULTS TO MEASURED DATA

Orienting the axes such that the x-direction is horizontal and the y-direction is vertical, the strain measured in the UTSA test at the center of the target plate is recorded in Table 2.

Orientation	Strain (Microns)	Strain (%)
x-axis	17.8	0.00178
y-axis	29.5	0.00295

Table 2 – *Measured Strain from the UTSA Test*

It is interesting to note that the strains in the horizontal and vertical directions are not identical as previously assumed. This can be due to various factors, including the approximations made about the plate dimensions. However, this does not account for the large variation in strain between the horizontal and vertical direction. This difference is partially due to the presence of the air pressure above the soil sample. This overburden pressure causes a variation in pressure on the face of the plate along a vertical line, which invalidates the assumption that pressure is uniform along the face of the plate. Since stress and strain were calculated in the horizontal plane, the discussion from this point will be limited to strain along this plane.

A comparison of the strains in the x-direction from the UTSA test to those calculated for Case 2 above (non-uniform pressure in the shape of a triangle) using the available equations yields the results found in Table 3.

Source	Strain (%)
UTSA Test	0.00178
Calculations	0.01542

Table 3 – *Comparison of the UTSA Test Results with Calculated Values*

There is a large degree of difference between the calculated results and those actually measured, approximately on an order of ten magnitude. More specifically, the calculated strain is nine times greater than the measured strain. Dr. Chen's research provided similar results. As mentioned earlier, his research developed a SDOF model to more accurately predict the developed free field stresses; as such, his SDOF model predicted stresses that were five times less than those predicted by Equation (1). Additionally, Dr. Chen's SDOF model was more accurate for predicting lower stresses on thin Plexiglas plates. The thicker the plate, the more variance between stresses predicted in the model and those actually measured, with the stresses predicted by the model always higher than the measured stresses. As a result, the measured free field stresses, which were not reported in Dr. Chen's study, were most likely less than those predicted by the SDOF model. Therefore, it can be deduced that the factor of five difference between the

predictions of the SDOF model and the measured data could easily be nearer the order of nine magnitude difference for the free field stresses that we discovered in our study.

Knowing that the measured strains were much smaller than those predicted by Equation (1), we can hazard a few guesses as to the reason behind these differences. One very simple suggestion is that the equation is far too simplified to be useful in predicting the free field pressure acting on the plate. The equation does not take into account the material properties of the medium through which the pressure is being transmitted. The Modulus of Elasticity, E, of the medium, which is the property which reflects how P-waves travel through a medium, does not enter into the equation. To illustrate, if you were to replace the sand medium with steel, the free field stresses and corresponding strain remain the same using Equation (1) at the same distance from the loading plate. This is intuitively incorrect.

Another possible reason for the variation in predicted versus actual strains rests in the fact that the overburden pressure introduced via the air bladder actually produces a lateral loading on the soil, which causes the plate to deflect before loading occurs. Additionally, the assumptions for the UTSA test may not be completely valid. For instance, the end conditions assumed in determining the bending of the target plate were not identical to those used in the experiment, and the load profile on the plate was assumed to be triangular in shape, which at best is a close approximation to the actual case.

Perhaps the most dominant factor contributing to the difference between predicted and measured strains is the neglect of the soil-plate interaction phenomenon. This is a complicated process which, in actuality, results in a reduction of the load on the plate. This is due in part to soil-arching within the medium, separation between the plate and the soil caused by reflected stress waves and different velocities of the waves in the soil and the target plate, and load relief due to the rigid body displacement of the target plate. All in all, soil-plate interaction phenomenon plays a large role in the variance between the UTSA test measured and calculated strain data.

CONCLUSION

This special project analyzed the ability to predict free field stresses within a soil sample subjected to impulse loading by applying a simplified equation (see Equation (1)). While it would be convenient to use such an equation, it has been shown that the actual stresses and ensuing strains on an underground structure are the result of a very complicated process that must be studied in much greater depth to understand and predict these stresses. For this reason, further analysis of this problem using finite-element analysis is currently underway by Dr. Sam Helwany at the University of Wisconsin at Milwaukee. Unfortunately, the larger Air Force study, of which the UTSA test was the first phase, has been canceled. Even so, it can be stated that the soil-structure interaction problem on an underground structure caused by an impulse loading is extremely complicated and deserves far greater consideration than can be rendered here.

REFERENCES

1. Beer, Ferdinand B. and Johnston, E. Russell, Jr., Mechanics of Materials, Second Edition, McGraw-Hill, Inc., 1992.

2. Blake, Alexander, Handbook of Mechanics, Materials, and Structures, John Wiley & Sons, Inc., 1985.

3. Chen, H.L.; Keer, L.M.; Lin, W. and Shah, S.P., "Low Velocity Impact of an Elastic Plate Resting on Sand," Journal of Applied Mechanics, Vol. 110, December 1998.

4. Chen, Hung-Liang (Roger) and Chen, Shen-En, "Dynamic Responses of Shallow-Buried Flexible Plates Subjected to Impact Loading," Journal of Structural Engineering, January 1996.

5. Das, Braja M., Principles of Geotechnical Engineering, Fourth Edition, PWS Publishing Co., 1998.

6. Das, Braja M., Principles of Soil Dynamics, PWS-Kent Publishing Company, Boston, 1993.

7. Fenster, S.K., and Ugural, A.C., Advanced Strength and Applied Elasticity, Third Edition, Prentice-Hall, Inc., 1995.

8. Gere, James M. and Timoshenko, Stephen P., Theory of Elastic Stability, McGraw-Hill Book Company, Inc., 1961.

9. Helwany, Sam; Bagley, Ronald; and Chowdhury, Asadul, "Dynamic Lateral Earth Pressure on Underground Structures," AFOSR Grant F49620-98-1-0109.

10. Johnson, John E. and Salmon, Charles G., Steel Structures, Design and Behavior, Second Edition, Harper & Row Publishers, 1980.

11. McCarthy, David F., Essentials of Soil Mechanics, Basic Geotechnics, Second Edition, Reston Publishing Co., 1982.

12. Reddy, J.N., Energy and Variational Methods in Applied Mechanics, John Wiley & Sons, Inc, 1984.

13. Sack, Ronald L., Structural Analysis, Mc-Graw Hill Book Company, 1984.

14. Timoshenko, S. and Woinowsky-Krieger, S., Theory of Plates and Shells, Second Edition, McGraw-Hill Book Company, 1959.

APPENDIX – CALCULATIONS/NOTATIONS

CALCULATIONS FROM THE UTSA LARGE-SCALE IMPULSE TEST

Free Field Stresses:

Equivalent Uniformly Distributed Loading Due to a Point Load Acting on an Elastic Half-Space:

$$q(t) = \frac{P(t)}{4a^2}$$

$$q(t) = \frac{3725 lbs}{4(5.75 in)^2}$$

$$q(t) = 28.17 psi$$

Free-field Stress at a Depth z from the Loading Plate:

$$\sigma_{f(t,z)} = q(t) \left[1 - \frac{z^3}{\left(a^2 + z^2\right)^{1.5}} \right]$$

$$\sigma_{f(t,z)} = 28.17 psi \left[1 - \frac{(29.75 in)^3}{\left((5.75 in)^2 + (29.75 in)^2\right)^{1.5}} \right]$$

$$\sigma_{f(t,z)} = 1.508 psi$$

Equivalent Burial Depth Due to Presence of 10 psi Overburden Air Pressure on Soil Sample:

$$\sigma = \gamma h$$

Rearranging the equation yields:

$$h = \frac{\sigma}{\gamma}$$

$$h = \frac{10\,psi}{\left(108\,\dfrac{lb}{ft^3} \times \dfrac{1ft^3}{(12in)^3}\right)}$$

$$h = 160in = 13.33\,ft$$

Application of Theory of Bending of Plates - Calculating Maximum Stress and Deflection for the Target Plate:

Case 7 – Simply Supported with Uniform Load

Maximum Stress:

$$\sigma_{max} = \frac{C_7 p L^2}{h^2}$$

$$\sigma_{max} = \frac{(.30)(1.508\,psi)(42in)^2}{(.50in)^2}$$

$$\sigma_{max} = 3192.13\,psi$$

Maximum Deflection:

$$\omega_{max} = \frac{K_7 p L^4}{Eh^3}$$

$$\omega_{max} = \frac{(.044)(1.508\,psi)(42in)^4}{(10x10^6\,psi)(.50in)^3}$$

$$\omega_{max} = .165in$$

Strain in the x-direction:

$$\varepsilon_x = \frac{\sigma_x(1-\upsilon)}{E}$$

$$\varepsilon_x = \frac{(3192.13\,psi)(1-.332)}{10x10^6\,psi}$$

$$\varepsilon_x = .00021323\frac{in}{in} = .021323\%$$

Case 11 – Simply Supported with Load in the Shape of a Triangular Prism

Maximum Stress:

$$\sigma_{max} = \frac{C_{11}pL^2}{h^2}$$

$$\sigma_{max} = \frac{(.217)(1.508\,psi)(42in)^2}{(.50in)^2}$$

$$\sigma_{max} = 2308.98\,psi$$

Maximum Deflection:

$$\omega_{max} = \frac{K_{11}pL^4}{Eh^3}$$

$$\omega_{max} = \frac{(.031)(1.508\,psi)(42in)^4}{(10x10^6\,psi)(.50in)^3} = .116in$$

Strain in the x-direction:

$$\varepsilon_x = \frac{\sigma_x(1-\upsilon)}{E}$$

$$\varepsilon_x = \frac{(2308.98\,psi)(1-.332)}{10x10^6\,psi}$$

$$\varepsilon_x = .0001542\frac{in}{in} = .01542\%$$

CALCULATIONS FROM DR. CHEN'S RESEARCH

Free Field Stresses:

Equivalent Uniformly Distributed Loading Due to a Point Load Acting on an Elastic Half-Space:

$$q(t) = \frac{P(t)}{4a^2}$$

$$q(t) = \frac{1727 lbs}{4(3.0in)^2}$$

$$q(t) = 47.97 psi$$

Free-field Stress at a Depth z from the Loading Plate:

$$\sigma_{f(t,z)} = q(t)\left[1 - \frac{z^3}{\left(a^2 + z^2\right)^{1.5}}\right]$$

$$\sigma_{f(t,z)} = 47.97 psi\left[1 - \frac{(3.0in)^3}{\left((3.0in)^2 + (3.0in)^2\right)^{1.5}}\right]$$

$$\sigma_{f(t,z)} = 31.01 psi$$

NOTATIONS USED IN PAPER/CALCULATIONS:

The following symbols are used in this paper:

a = radius of the loading plate (in)

C_n = variable for calculating maximum stress on the target plate

E = Young's Modulus of Elasticity (psi)

$f(t)$ = loading function

g = gravitational acceleration (ft/sec^2)

h = equivalent height of overburden soil sample (in)

h = thickness of aluminum target plate (in)

H = dropping height of impactor (in)

K_n = variable for calculating maximum deflection on the target plate

L = span of the target plate (in)

M_o = mass of steel ball (lb)

P_o = peak amplitude of loading (lbs)

$P(t)$ = amplitude of impact loading (lbs)

$q(t)$ = uniform equivalent load (psi)

t = time (msec)

To = loading duration (msec)

z = distance from loading plate (in)

ε_x = strain in the horizontal direction (in/in)

γ = unit weight of the soil (lb/ft^3)

$\sigma_{f(t,z)}$ = free field stress at a given time and distance (psi)

σ_{max} = maximum stress on the target plate (psi)

ρ = density of soil sample (lb/ft^3)

υ = Poisson's Ratio

ω_{max} = maximum deflection of the target plate (in)